

Amplitude analysis of reaction $K^+ n_{\uparrow} \rightarrow K^+ \pi^- p$ at 5.98 GeV/c

M. Svec

*Physics Department, Dawson College, Montreal, Quebec, Canada H3Z 1A4
and McGill University, Montreal, Quebec, Canada H3A 2T8*

A. de Lesquen and L. van Rossum

Département de Physique des Particules Élémentaires, Centre d'Études Nucléaires, Saclay, France

(Received 10 June 1991)

We present a model-independent amplitude analysis of the reaction $K^+ n_{\uparrow} \rightarrow K^+ \pi^- p$ at 5.98 GeV/c using Saclay data obtained with a transversely polarized deuteron target at the CERN Proton Synchrotron. The analysis makes use of the data in two sets of binnings to examine the dependence of amplitudes on momentum transfer t [$-t \leq 1.0$ (GeV/c)²] in the K^{*0} mass region, and their dependence on $K^+ \pi^-$ invariant mass below 1000 MeV for momentum transfers $-t = 0.2-0.4$ (GeV/c)². The analysis is performed in both t -channel and s -channel helicity frames of the dimeson state. The data yield two solutions for 8 moduli and 6 cosines of relative phases of nucleon transversity amplitudes with dimeson spins $J=0$ (S wave) and $J=1$ (P wave). The two solutions differ mainly in the contributions of the S wave. Both solutions require nonzero nucleon helicity-flip amplitudes. The differences in the moduli of the amplitudes with a recoil nucleon transversity "up" and "down" reveal the essential role of nucleon spin in the pion production process. The P -wave moduli show unexpected structures within the K^{*0} mass range which provide new information on K^{*0} production. The mass dependence of solution 2 suggests the possible existence of a scalar state $I = \frac{1}{2} 0^+$ (887) with a width of about 20 MeV. We comment on its possible constituent structure. Our results emphasize the need for a systematic study of pion production on the level of amplitudes in a new generation of dedicated experiments with spin at the recently proposed advanced hadron facilities.

PACS number(s): 13.88.+e, 13.75.Jz, 14.40.Ev

I. INTRODUCTION

Two-body scattering experiments with definite initial or final spin states of interacting hadrons provide complete sets of observables which enable construction of the scattering amplitudes directly from experimental data. Such a model-independent determination of amplitudes is known as amplitude analysis.

Measurements of three-body final states produced in meson-nucleon scattering on polarized targets yield in a single experiment enough observables that almost complete amplitude analysis can be performed in the kinematic region with dimeson masses below 1000 MeV. The results enable us to study the resonance production on the level of production amplitudes, the dependence of exchange amplitudes with definite dimeson and nucleon spin states on the dimeson mass, and the contributions from unnatural exchange amplitudes with t -channel quantum numbers not exchanged in simple meson-nucleon two-body scattering.

The first measurement of the reaction $K^+ n_{\uparrow} \rightarrow K^+ \pi^- p$ on transversely polarized quasifree neutrons was carried out by Saclay group at the CERN Proton Synchrotron (PS) using the CERN polarized deuteron target. The experimental apparatus [1,2] was designed primarily for the measurement of polarization in $K^+ n_{\uparrow} \rightarrow K^0 p$ [1-6] but the data acquisition was triggered also on several other channels with incident pions and kaons at $p_{\text{lab}} = 5.98$ and 11.85 GeV/c: $\pi^+ p_{\uparrow} \rightarrow \pi^+ p$ and $K^+ p_{\uparrow} \rightarrow K^+ p$ [7],

$\pi^+ n_{\uparrow} \rightarrow \pi^0 p$ [8], $\pi^+ n_{\uparrow} \rightarrow \pi^+ \pi^- p$ [9-12] and $K^+ n_{\uparrow} \rightarrow K^+ \pi^- p$ [9,11,13,14].

The data for $K^+ n_{\uparrow} \rightarrow K^+ \pi^- p$ cover the kinematic region of the four-momentum transfer squared $-t = 0.1-1.0$ (GeV/c)² and of the $K^+ \pi^-$ invariant mass $m = 812-972$ MeV. The data analysis was published in Ref. [14]. It used 12 000 events at 5.98 GeV/c and 2000 events at 11.85 GeV/c. In each (m, t) bin the experiment yields average values of 14 spin-density-matrix (SDM) elements describing the coherent production of $K^+ \pi^-$ states with dimeson spins $J=0$ (S wave) and $J=1$ (P wave). Three sets of (m, t) binnings were used at $p_{\text{lab}} = 5.98$ GeV/c. The first two sets

$$0.1 \leq -t \leq 1.0 \text{ (GeV/c)}^2 \text{ with } m = 842-942 \text{ MeV} \quad (1.1)$$

and

$$812 \leq m \leq 972 \text{ MeV with } -t = 0.2-0.4 \text{ (GeV/c)}^2 \quad (1.2)$$

provide information about the t dependence of pion production in the K^{*0} mass region and about its dependence on the dimeson mass m in the interval of $-t$ with the highest statistics. The third set of binnings covers the entire kinematic region accessible by the experiment. The data analyses were performed independently in both s - and t -channel dimeson helicity frames of reference.

The measured polarized SDM elements enable a model-independent amplitude analysis which provides moduli of the production amplitudes and cosines of certain relative phases between the amplitudes. Various aspects of the amplitude analysis of the reaction $\pi^+n_{\uparrow} \rightarrow \pi^+\pi^-p$ were published [15–22] including details of the formalism and the method of amplitude analysis [22]. In this paper we present the results of the amplitude analysis of $K^+n_{\uparrow} \rightarrow K^+\pi^-p$ at 5.98 GeV/c in the (m, t) binnings (1.1) and (1.2). This amplitude analysis provides the first model-independent separation of the S -wave and P -wave contributions to the pion production in this reaction on the level of amplitudes as well as the separation of partial-wave intensities and polarizations. The analysis looks at both the t dependence in the K^{*0} mass range and the dimeson mass dependence for $-t=0.2-0.4$ (GeV/c)² of all these quantities. To facilitate model building with the necessary data we perform the analysis in both s -channel and t -channel dimeson helicity frames of reference. Our results bring entirely new information on pion production in the reaction $K^+n_{\uparrow} \rightarrow K^+\pi^-p$ and contribute to the study of hadron dynamics at intermediate energies.

Preliminary results [15] and numerical tables with final results [23] appeared earlier elsewhere. We have used the results of the amplitude analysis to test the additive quark model on the level of amplitudes [24] and confirmed its validity. The third set of binnings was used to study the evolution of t dependence of bounds on the moduli squared of 8 amplitudes describing the $K^+\pi^-$ production [21].

The paper is organized in four sections. In Sec. II we summarize the necessary formalism to introduce our notation. In Sec. III we present our results and discussion. Section IV closes the paper with a summary.

II. BASIC FORMALISM

The formalism describing the kinematics, observables, amplitudes and relations between observables and amplitudes in the case of $J=0$ and $J=1$ dimeson production in reactions $\pi N \rightarrow \pi\pi N$ and $KN \rightarrow K\pi N$ was presented in detail in Refs. [14,22,25]. Extensions for $J \geq 2$ were also studied [25,26]. Here we only outline some aspects of the formalism to set our notation for the presentation and discussion of our results.

Experiments on a transversely polarized target measure the following spin-density-matrix (SDM) elements for dimeson masses below 1000 MeV:

$$\rho_{ss} + \rho_{00} + 2\rho_{11}, \rho_{1-1}, \rho_{00} - \rho_{11}, \quad (2.1a)$$

$$\text{Re}\rho_{10}, \text{Re}\rho_{1s}, \text{Re}\rho_{0s},$$

$$\rho_{ss}^y + \rho_{00}^y + 2\rho_{11}^y, \rho_{1-1}^y, \rho_{00}^y - \rho_{11}^y, \quad (2.1b)$$

$$\text{Re}\rho_{10}^y, \text{Re}\rho_{1s}^y, \text{Re}\rho_{0s}^y,$$

$$\text{Im}\rho_{1-1}^x, \text{Im}\rho_{10}^x, \text{Im}\rho_{1s}^x. \quad (2.1c)$$

The SDM elements in (2.1a) are also measured in experiments on unpolarized targets. The observables in (2.1b) and (2.1c) are determined by the transverse com-

ponent of target polarization perpendicular and parallel to the scattering plane of $KN \rightarrow (K\pi)N$, respectively. In the Saclay experiment the polarization component in the scattering plane (perpendicular to incident momentum) was small and the SDM elements (2.1c) were thus measured with a lesser precision than the SDM elements in (2.1b).

The $K^+\pi^-$ system is not produced, in general, in the state of definite spin, helicity, and parity. The reaction $K^+n \rightarrow K^+\pi^-p$ is described by pion production amplitudes $H_{\lambda_p, 0\lambda_n}(s, t, m, \theta, \phi)$ where λ_p and λ_n are the helicities of the proton and neutron, respectively. The pion production amplitudes can be expressed in terms of pion production amplitudes corresponding to definite dimeson spin J using an angular expansion

$$H_{\lambda_p, 0\lambda_n} = \sum_{J=0}^{\infty} \sum_{\lambda=-J}^{+J} (2J+1)^{1/2} \times H_{\lambda\lambda_p, 0\lambda_n}^J(s, t, m) d_{\lambda 0}^J(\theta) e^{i\lambda\phi}, \quad (2.2)$$

where J is the spin and λ is the helicity of the $K^+\pi^-$ dimeson system. The ‘‘partial wave’’ amplitudes $H_{\lambda\lambda_p, 0\lambda_n}^J$ can be expressed in terms of nucleon helicity amplitudes with definite t -channel-exchange naturality. In the case when the $K^+\pi^-$ system is produced in the S - and P -wave states we have

$$0^{-\frac{1}{2}+} \rightarrow 0^{+\frac{1}{2}+}, \quad H_{0+, 0+}^0 = S_0,$$

$$H_{0+, 0-}^0 = S_1, \quad (2.3a)$$

$$0^{-\frac{1}{2}+} \rightarrow 1^{-\frac{1}{2}+}, \quad H_{0+, 0+}^1 = L_0,$$

$$H_{0+, 0-}^1 = L_1,$$

$$H_{\pm 1+, 0+}^1 = \frac{N_0 \pm U_0}{\sqrt{2}},$$

$$H_{\pm 1+, 0-}^1 = \frac{N_1 \pm U_1}{\sqrt{2}}. \quad (2.3b)$$

At large s , the amplitudes N_0 and N_1 are both dominated by natural ‘‘ $A_2-\rho$ ’’ exchange. The amplitudes $S_n, L_n, U_n, n=0,1$ are dominated by unnatural exchanges: ‘‘ A_1-Z ’’ for $n=0$ and ‘‘ $\pi-B$ ’’ for $n=1$. The index $n=|\lambda_n-\lambda_p|=0,1$ is nucleon helicity flip. The ‘‘ Z ’’ and ‘‘ B ’’ exchange quantum numbers correspond to isovectors with $J^{PC}=2^{--}$ and 1^{+-} , respectively.

The data on the transversely polarized target are best analyzed in terms of nucleon transversity amplitudes (NTA’s) [14,22,25]. In our kinematic region we work with two S -wave and six P -wave NTA’s of definite naturality defined as [14,22,25]

$$S = (S_0 + iS_1)/2^{1/2}, \quad \bar{S} = (S_0 - iS_1)/2^{1/2},$$

$$L = (L_0 + iL_1)/2^{1/2}, \quad \bar{L} = (L_0 - iL_1)/2^{1/2},$$

$$U = (U_0 + iU_1)/2^{1/2}, \quad \bar{U} = (U_0 - iU_1)/2^{1/2},$$

$$N = (N_0 - iN_1)/2^{1/2}, \quad \bar{N} = (N_0 + iN_1)/2^{1/2}. \quad (2.4)$$

The amplitudes S, L, U, N and $\bar{S}, \bar{L}, \bar{U}, \bar{N}$ correspond to recoil nucleon transversity ‘‘down and ‘‘up,’’ respectively. The S -wave amplitudes S, \bar{S} and P -wave amplitudes L, \bar{L} have dimeson helicity $\lambda=0$. The pairs of amplitudes U, \bar{U}

and N, \bar{N} are combinations of nucleon helicity amplitudes with dimeson helicities $\lambda = \pm 1$ and have opposite t -channel-exchange naturality. While the amplitudes S, \bar{S}, L, \bar{L} and U, \bar{U} are nucleon transversity flip amplitudes, the amplitudes N, \bar{N} are nucleon transversity nonflip.

In our normalization, the integrated cross section $\Sigma \equiv d^2\sigma/dm dt$ is given by

$$\begin{aligned} \Sigma &= \sum_{n=0,1} |S_n|^2 + |L_n|^2 + |U_n|^2 + |N_n|^2 \\ &= |S|^2 + |\bar{S}|^2 + |L|^2 + |\bar{L}|^2 + |U|^2 + |\bar{U}|^2 + |N|^2 + |\bar{N}|^2. \end{aligned} \quad (2.5)$$

In the Saclay experiment the cross section was not measured. Consequently, we will work with normalized amplitudes corresponding to

$$\Sigma = d^2\sigma/dm dt \equiv 1. \quad (2.6)$$

The determination of moduli squared of NTA (2.4) in our amplitude analysis allows us to construct partial-wave cross sections $\sigma(A)$ and partial-wave polarizations $\tau(A)$ defined for amplitudes $A = S, L, U, N$ as

$$\begin{aligned} \sigma(A) &= |A_0|^2 + |A_1|^2 = |A|^2 + |\bar{A}|^2, \\ \tau(A) &= 2\epsilon \operatorname{Im}(A_0 A_1^*) = |A|^2 - |\bar{A}|^2, \end{aligned} \quad (2.7)$$

where $\epsilon = +1$ for $A = S, L, U$ and $\epsilon = -1$ for $A = N$. In our normalization the reaction cross section is

$$\Sigma = \sigma(S) + \sigma(L) + \sigma(U) + \sigma(N) = 1. \quad (2.8)$$

Before we present and discuss our results, we shall note several relations between the moduli of nucleon transversity amplitudes $|A|^2$ and $|\bar{A}|^2$, and the moduli of nucleon helicity amplitudes $|A_0|^2$ and $|A_1|^2$ which will be useful for their physical interpretation.

From (2.4) we obtain

$$\begin{aligned} 2|A|^2 &= |A_0|^2 + |A_1|^2 + 2\epsilon |A_0| |A_1| \sin(\phi_0 - \phi_1), \\ 2|\bar{A}|^2 &= |A_0|^2 + |A_1|^2 - 2\epsilon |A_0| |A_1| \sin(\phi_0 - \phi_1), \end{aligned} \quad (2.9)$$

where $\epsilon = +1$ for $A = S, L, U$ and $\epsilon = -1$ for $A = N$. ϕ_0 and ϕ_1 are phases of helicity amplitudes A_0 and A_1 , respectively. It follows from (2.9) that when

$$|A| \neq |\bar{A}| \text{ then } |A_0| \neq 0, |A_1| \neq 0, \text{ and } \phi_0 - \phi_1 \neq 0. \quad (2.10)$$

In particular, when one of the moduli of transversity amplitudes A and \bar{A} is zero or small, the modulus of the amplitude with opposite transversity attains its maximum or near maximum value. When

$$|A| = |\bar{A}| \text{ then either } |A_0| \text{ or } |A_1| = 0 \quad (\text{but not both}), \text{ or } \phi_0 - \phi_1 = 0. \quad (2.11)$$

Note that $|A_0| = |A_1| = 0$ only when $|A| = |\bar{A}| = 0$. The partial-wave polarization defined in (2.7),

$$\tau(A) = |A|^2 - |\bar{A}|^2 = 2\epsilon |A_0| |A_1| \sin(\phi_0 - \phi_1), \quad (2.12)$$

determines the sign of relative phase $\phi_0 - \phi_1$. A crossover of moduli $|A|$ and $|\bar{A}|$ of transversity amplitudes gives rise to a change of sign in τ and in the relative phase of the corresponding helicity amplitudes. The ambiguity in (2.11) cannot be resolved when the polarization τ has a zero without change of sign (a double zero). It is also possible to show [22] that when

$$|A| \text{ or } |\bar{A}| = 0 \text{ then } |A_0| = |A_1|. \quad (2.13)$$

III. RESULTS AND DISCUSSION

The amplitude analysis of the reaction $K^+ n_1 \rightarrow K^+ \pi^- p$ was done using the same method we used for the analysis of reaction $\pi^+ n_1 \rightarrow \pi^+ \pi^- p$ and described in Ref. [22].

The SDM elements (2.1) were measured at 5.98 and 11.85 GeV/c but, because of low statistics at 11.85 GeV/c, we have performed the amplitude analysis only at 5.98 GeV/c. The analysis was carried out for the two sets of binnings (1.1) and (1.2) with 7 t bins in (1.1) and 8 mass bins in (1.2). In each case the analysis was performed in both s - and t -channel helicity frame for the dimeson system.

The SDM elements (2.1a) and (2.1b) organize themselves into two independent groups corresponding to their sum and difference [22]. The first group (sum) involves the following moduli of normalized NTA and cosines of relative phases:

$$\begin{aligned} &|S|^2, |L|^2, |U|^2, |\bar{N}|^2, \\ &\cos(\gamma_{SL}), \cos(\gamma_{SU}), \cos(\gamma_{LU}). \end{aligned} \quad (3.1)$$

The second group (differences) involves amplitudes of opposite transversity:

$$\begin{aligned} &|\bar{S}|^2, |\bar{L}|^2, |\bar{U}|^2, |N|^2, \\ &\cos(\bar{\gamma}_{SL}), \cos(\bar{\gamma}_{SU}), \cos(\bar{\gamma}_{LU}). \end{aligned} \quad (3.2)$$

In each (m, t) bin our analysis yields two solutions for amplitudes (3.1) and (3.2). One of the solutions provides P -wave moduli which are always larger than the moduli in the second solution. We label the larger and smaller solutions as solution 1 and solution 2, respectively. In some (m, t) bins we obtain two complex conjugate solutions. In such a case we accept their real part as an approximate double solution which we label solution 0.

In the following figures the results for solution 1 and 2 are represented by the symbols \dagger and \blacklozenge respectively. Solution 0 is represented by symbol \circ without error bars. The errors on Solution 0 are comparable to nearby real solutions. The figures for cosines do not show some results with unphysical values.

The solutions for amplitudes in (3.1) and (3.2) are entirely independent. We can denote the two solutions for normalized NTA's as $A(i)$ and $\bar{A}(j)$ with $i = 1, 2$ and $j = 1, 2$. Because the moduli in (3.1) and (3.2) are independent, there is a fourfold ambiguity in the partial-wave cross sections and polarizations. Using the indices i and j to label the four solutions, we get

$$\sigma(A) \equiv \sigma_A(i,j) = |A(i)|^2 + |\bar{A}(j)|^2, \quad (3.3)$$

$$\tau(A) \equiv \tau_A(i,j) = |A(i)|^2 - |\bar{A}(j)|^2.$$

There are four solutions for the unnormalized partial-wave cross sections

$$I_A(i,j) = \sigma_A(i,j)\Sigma, \quad (3.4)$$

where Σ is the reaction cross section.

A. t Dependence of solutions in the mass region of K^{*0} resonance

Our results for the moduli of normalized nucleon transversity amplitudes and the cosines of the relative phases in the kinematic region $0.1 \leq |t| \leq 1.0$ (GeV/c)² and averaged over the dimeson mass interval $842 \leq m \leq 942$ MeV are shown in Fig. 1. The figure shows

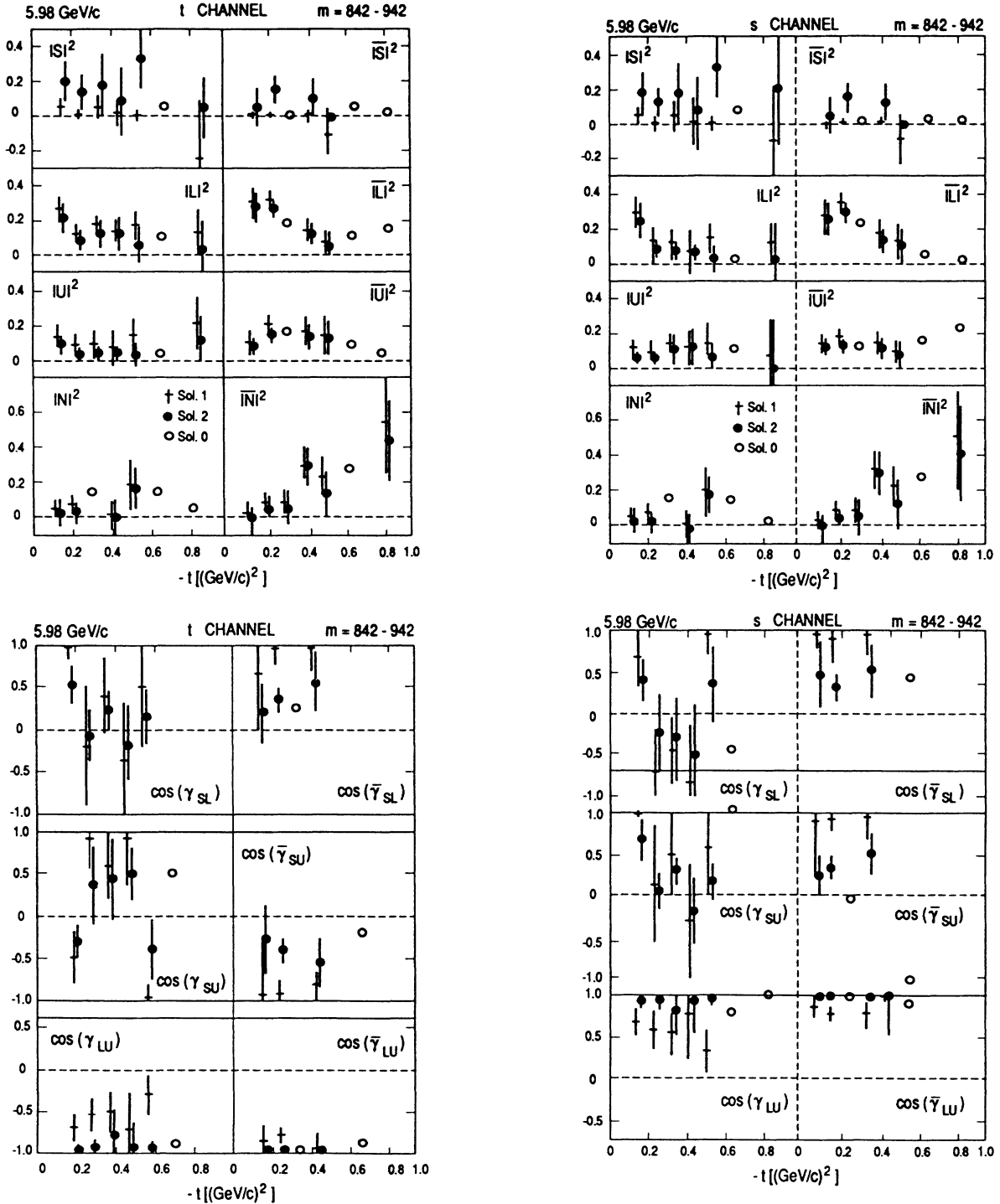


FIG. 1. The t dependence of moduli squared of normalized nucleon transversity amplitudes and cosines of their relative phases for dimeson masses in the K^{*0} mass region $m = 842 - 942$ MeV at a K^+ incident momentum of 5.98 GeV/c. The figure shows results in dimeson t - and s -channel helicity frames. The symbols \dagger , \bullet and \circ denote solution 1, solution 2 and solution 0 (real part of complex solution), respectively.

the results for both t - and s -channel helicity frames of the dimeson state.

First we notice that the two solutions for P -wave moduli are very close and show the same structures as a function of t . The largest differences are in the S wave where solution 2 for $|S|^2$ and $|\bar{S}|^2$ is comparable in magnitude to P -wave moduli but solution 1 is small and consistent with zero for $|\bar{S}|^2$. The amplitudes $|S|^2$, $|\bar{S}|^2$, $|N|^2$, $|\bar{N}|^2$ are helicity frame invariant. The comparison of these moduli in the t and s channels shows essentially the same behavior. This result is an important self-consistency test of our amplitude analysis.

Next we observe that the pion production is dominated by the amplitudes with recoil nucleon spin "up". In particular, the pion production is dominated by the amplitude $|\bar{L}|^2$ for $-t \lesssim 0.4$ (GeV/c)² and by $|\bar{N}|^2$ for $-t \gtrsim 0.4$ (GeV/c)². Similar behavior was observed in the reaction $\pi^+ n \rightarrow \pi^+ \pi^- p$ in the same kinematic region of $-t$ with masses in the ρ^0 mass region [22]. It is not obvious why both pion creation processes proceed predominantly with recoil nucleon spin "up" in the resonance region, and why both processes are dominated by nucleon transversi-

ty flip amplitude $|\bar{L}|^2$ (with $\lambda=0$) for $-t \lesssim 0.4$ (GeV/c)² and nucleon transversity nonflip amplitude $|\bar{N}|^2$ (with $\lambda=\pm 1$) for $-t \gtrsim 0.4$ (GeV/c)².

The cosines of relative phases show several interesting features. Solution 2 for $\cos\gamma_{LU}$ and $\cos\bar{\gamma}_{LU}$ indicates that the pairs of amplitudes L, U and \bar{L}, \bar{U} are 180° out of phase in the t channel but are nearly 0° in phase in the s channel. Solution 1 also shows a sign-inversed behavior. We note that $\cos\gamma_{SL}$ and $\cos\bar{\gamma}_{SL}$ in the t channel resemble $\cos\gamma_{SU}$ and $\cos\bar{\gamma}_{SU}$ in the s channel. Similarly, $\cos\gamma_{SU}$ and $\cos\bar{\gamma}_{SU}$ in the t channel resemble sign-inversed $\cos\gamma_{SL}$ and $\cos\bar{\gamma}_{SL}$ in the s channel. In both s and t channels, $\cos\gamma_{SL}=0$ and $\cos\gamma_{SU}=0$ near $t \simeq -0.5$ (GeV/c)². This behavior is not seen in $\cos\bar{\gamma}_{SL}$ and $\cos\bar{\gamma}_{SU}$.

Figure 2 shows the partial-wave polarizations $\tau_A(1,2)$ and $\tau_A(2,1)$, also in both t - and s -channel helicity frames. The solutions $\tau_A(1,1)$ and $\tau_A(2,2)$ are within the bounds of $\tau_A(1,2)$ and $\tau_A(2,1)$ and show a similar behavior.

We notice the $\tau_S(1,2)$ is mostly negative while $\tau_S(2,1)$ is positive. This implies that $\tau_S(1,2)$ and $\tau_S(2,1)$ are dominated by recoil transversity "up" and "down" amplitudes $|\bar{S}|^2$ and $|S|^2$, respectively. Next we notice a

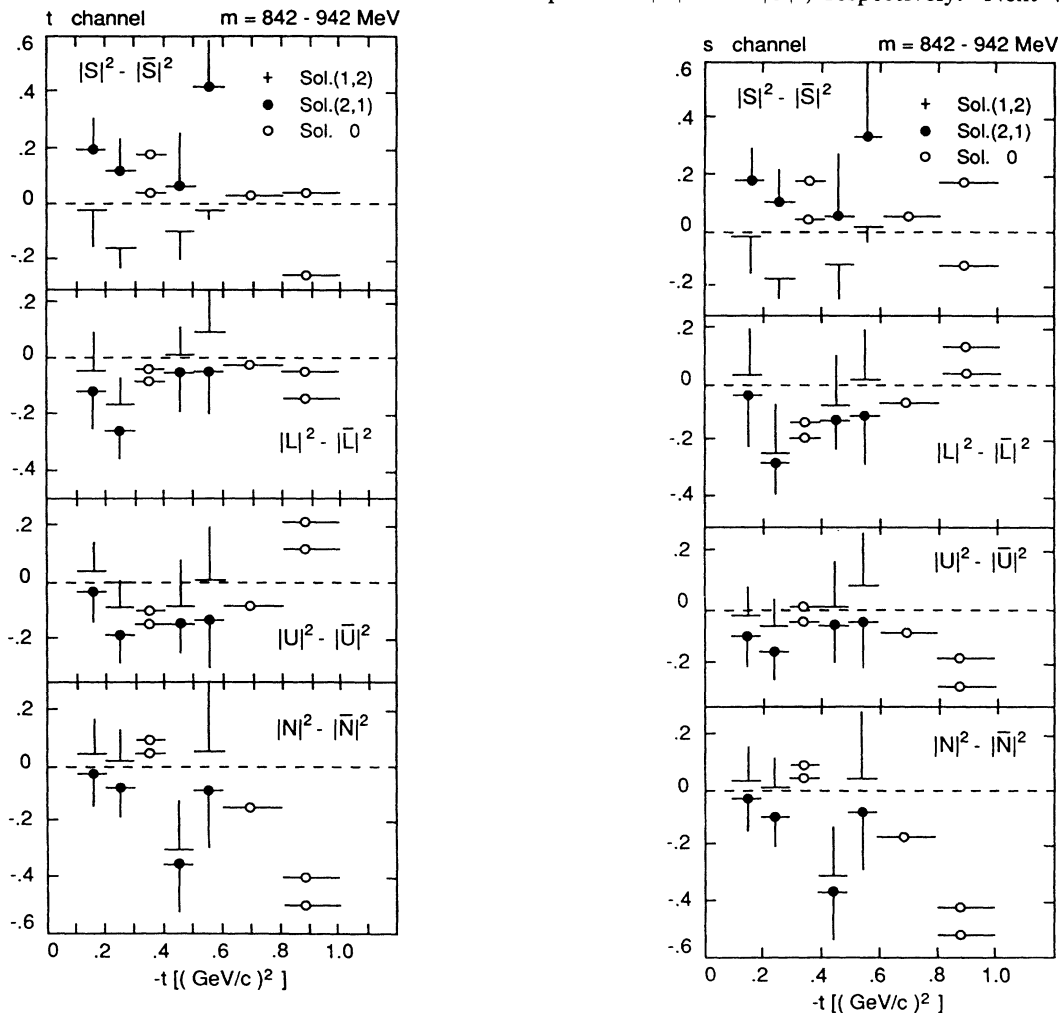


FIG. 2. The t dependence of partial-wave recoil nucleon polarizations τ in the K^{*0} mass region $m = 842 - 942$ MeV at an incident K^+ momentum of 5.98 GeV/c in the dimeson t - and s -channel helicity frames. Symbols as in Fig. 1.

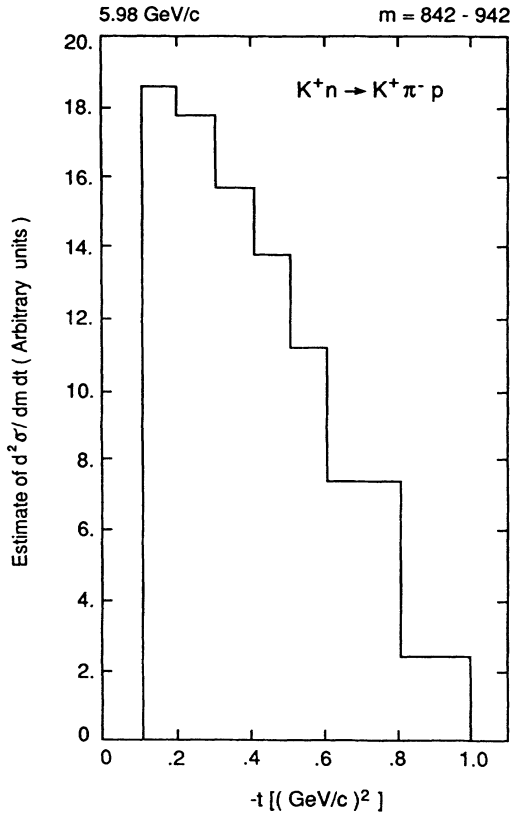


FIG. 3. Approximate results for t dependence of the unpolarized cross section of $K^+n \rightarrow K^+\pi^-p$ at 5.98 GeV/c. The units are arbitrary.

pronounced dip in τ_L at $-t \approx 0.25$ (GeV/c) 2 . The generally negative values of τ_L for $-t \lesssim 0.8$ (GeV/c) 2 correspond to the dominance of the $|\bar{L}|^2$ amplitude. The polarization τ_U is generally negative but has smaller magnitudes than τ_L at smaller $-t$. The large difference in the moduli $|A|^2$ and $|\bar{A}|^2$ for $A = S, L, U$ is evidence for the large and nontrivial contribution from the nucleon helicity-nonflip amplitudes which are dominated by “ A_1 -Z” exchange. These contributions depend on the meson spin and helicity. The difference between τ_S, τ_L , and τ_U in the reaction $K^+n \rightarrow K^+\pi^-p$ (Fig. 2) and in the reaction $\pi^+n \rightarrow \pi^+\pi^-p$ (Fig. 3 of Ref. [22]) indicate clear evidence for the “Z”-exchange contribution in $K^+n \rightarrow K^+\pi^-p$ with quantum numbers $I^G = 1^-, J^{PC} = 2^{--}$. Only “ A_1 ” exchange contributes to helicity-nonflip amplitudes in the reaction $\pi^+n \rightarrow \pi^+\pi^-p$.

A pronounced feature of τ_N is its large negative value at $-t \approx 0.45$ (GeV/c) 2 for all solutions. This behavior contrasts with τ_N in $\pi^+n \rightarrow \pi^+\pi^-p$ which shows a linear decrease for $-t \gtrsim 0.3$ (GeV/c) 2 and is zero at $-t \approx 0.45$ (GeV/c) 2 (see Fig. 3 in Ref. [22]). Both amplitudes $|N|^2$ and $|\bar{N}|^2$ are dominated by A_2 exchange in $\pi^+n \rightarrow \pi^+\pi^-p$ and by A_2 - ρ exchange in $K^+n \rightarrow K^+\pi^-p$. The remarkable differences at $t \approx 0.45$ (GeV/c) 2 in both reactions are due to ρ -exchange contribution in $K^+n \rightarrow K^+\pi^-p$.

It is of interest to construct also the unnormalized amplitudes $|A|^2\Sigma$ and $|\bar{A}|^2\Sigma$ and unnormalized partial-wave cross sections $I_A = \sigma_A\Sigma$. In Fig. 3 we present our estimate of the acceptance corrected reaction cross section $d^2\sigma/dm dt$ which we use for Σ .

Figure 4 shows the unnormalized moduli squared in the t -channel helicity frame. A notable feature is the similarity of P -wave moduli both in structure and magnitude, and considerable difference between solutions 1 and 2 for both S -wave moduli. Next we notice that the real parts of the complex solutions fit smoothly into the behavior of P -wave moduli. This suggests that the dip in solution 2 for $|\bar{S}|^2\Sigma$ at $-t \approx 0.35$ (GeV/c) 2 is a real effect. The amplitude $|L|^2\Sigma$ shows a clear dip at $-t \approx 0.25$ (GeV/c) 2 while $|\bar{L}|^2\Sigma$ has a smooth behavior and clearly dominates the pion production at small $-t \lesssim 0.3$ (GeV/c) 2 . The amplitude $|\bar{U}|^2\Sigma$ peaks at $-t \approx 0.25$ (GeV/c) 2 indicating a strong contribution from the nucleon helicity-flip amplitude U_1 . In contrast, the amplitude $|U|^2\Sigma$ is smaller and without evident structures.

A remarkable feature of natural exchange transversity nonflip amplitudes $|N|^2\Sigma$ and $|\bar{N}|^2\Sigma$ is their behavior at $-t \approx 0.45$ (GeV/c) 2 where $|N|^2\Sigma$ is small or vanishes while $|\bar{N}|^2\Sigma$ clearly peaks. In terms of nucleon helicity amplitudes, this behavior corresponds to $|N_0| = |N_1|$ and the $\sin(\phi_{N_0} - \phi_{N_1}) \approx 1$ at this value of t [Eq. (2.13)]. This value of t is also special in the reaction $\pi^+n \rightarrow \pi^+\pi^-p$. There the amplitudes $|N|^2\Sigma$ and $|\bar{N}|^2\Sigma$ show a crossover implying that either $|N_0|$ or $|N_1|$ vanishes, or that $\sin(\phi_{N_0} - \phi_{N_1}) \approx 0$ at $-t \approx 0.45$ (GeV/c) 2 .

In Fig. 5 we show unnormalized partial-wave cross sections. The two presented solutions $I_A(1,1)$ and $I_A(2,2)$, $A = S, L, U, N$ are extreme values within which are the two additional solutions $I_A(1,2)$ and $I_A(2,1)$. Even when only one of the amplitudes $|A|^2$ or $|\bar{A}|^2$ has a complex solution, we label the corresponding value of I_A with the complex solution symbol \circ , and take it accordingly as a part of $I_A(1,1)$ or $I_A(2,2)$. We note that these “complex solutions” still fit very smoothly into the behavior of P -wave cross sections. This suggests that real solutions at these values of t would not be far off also for the S -wave cross section I_S .

The S -wave cross section $I_S(1,1)$ is relatively small and rather flat. In contrast, $I_S(2,2)$ is a large contribution to Σ and it may have a dip at $-t \approx 0.35$ (GeV/c) 2 due to the dip in $|\bar{S}|^2\Sigma$. Such a large difference between the two solutions for I_S is not seen in $\pi^+n \rightarrow \pi^+\pi^-p$ at the same energy in ρ^0 mass region (Fig. 4 in Ref. [22]) where $I_S(2,2)$ is comparable to $I_S(1,1)$ and is also showing a rather flat shape.

The P -wave cross section I_L is the largest contribution to Σ at small $-t$. It decreases monotonically with t and is hiding the dip in $|L|^2\Sigma$ at $-t \approx 0.25$ (GeV/c) 2 . In both solutions its slope is smaller than the steep slope of I_L in the reaction $\pi^+n \rightarrow \pi^+\pi^-p$ (Ref. [22]) which is dominated by pion exchange for $-t \lesssim 0.3$ (GeV/c) 2 .

The cross sections I_U and I_N measure the contributions with meson helicities $\lambda = \pm 1$. Their notable feature is a turnover with a peak at $-t \approx 0.25 - 0.35$ (GeV/c) 2 for I_U and broader peak at $-t \approx 0.45 - 0.55$

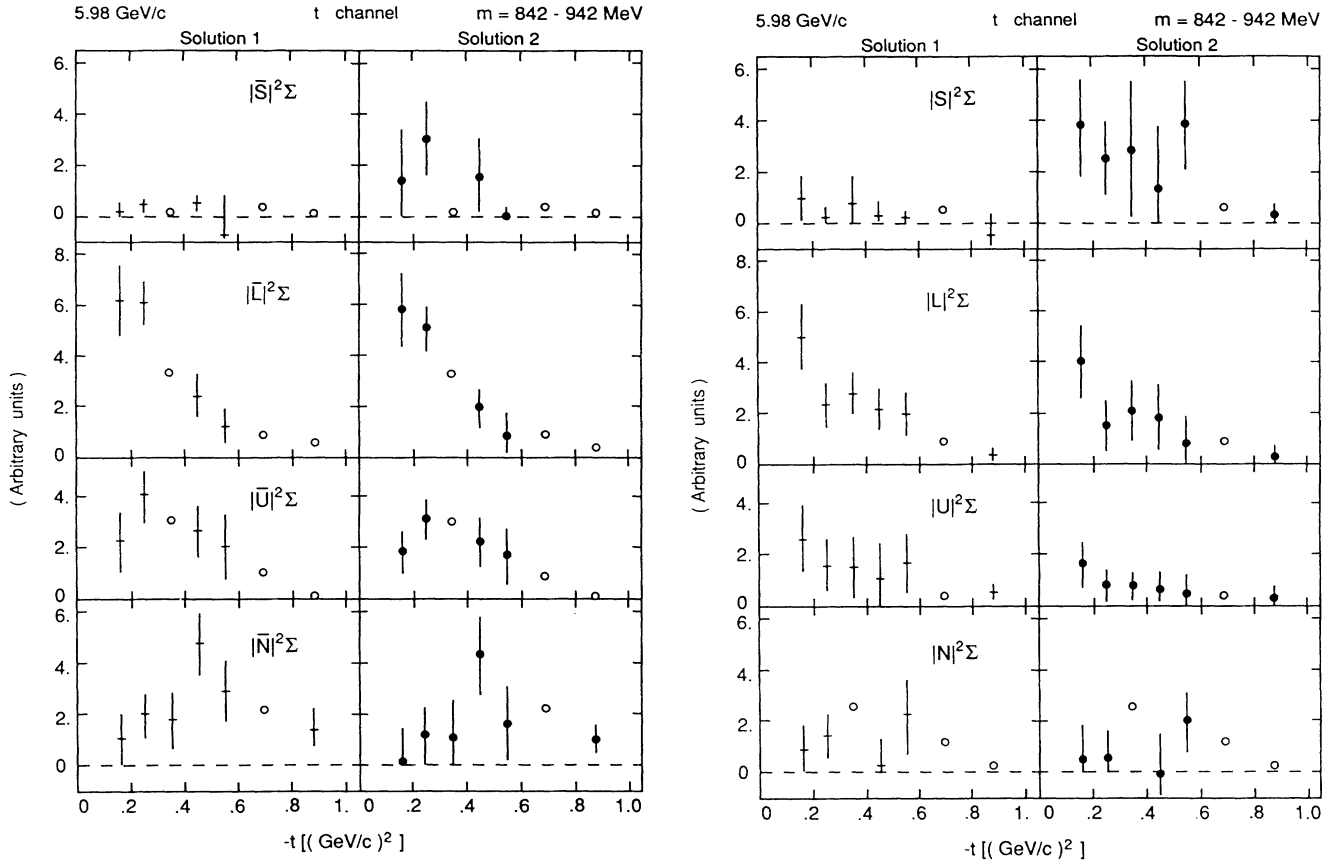


FIG. 4. The t dependence of moduli squared of unnormalized nucleon transversity amplitudes for dimeson masses $m = 842 - 942$ MeV in the t -channel helicity frame at K^+ incident momentum of 5.98 GeV/c. Symbols as in Fig. 1. The units as in Fig. 3.

(GeV/c)² for I_N . This behavior of the unnatural-exchange cross section I_U differs from that of I_U in the reaction $\pi^+ n \rightarrow \pi^+ \pi^- p$ (Fig. 4 in Ref. [22]) which sharply peaks at $-t \simeq 0.15$ (GeV/c)² and is relatively small for $-t \gtrsim 0.3$ (GeV/c)². The natural exchange cross sections I_N are similar in both reactions. In particular, they both peak near $-t \simeq 0.45$ (GeV/c)².

We may also compare our results for the P -wave cross sections I_L , I_U and I_N with the model-dependent results obtained in measurements of $K^+ n \rightarrow K^+ \pi^- p$ on an unpolarized target at 6 GeV/c at the Argonne Zero Gradient Synchrotron (Ref. [27], Figs. 32, 33, and 35). The Argonne analysis treats the S -wave contribution as a small background in our range of t . There is a qualitative agreement in the shape and slope of the $\lambda = 0$ cross sections I_L but a marked disagreement between the $|\lambda| = 1$ cross sections I_U and I_N . In the Argonne analysis these cross sections are structureless and slowly decrease with t . In contrast, our analysis yields I_U and I_N which make a larger contribution to the reaction cross section Σ (up to a factor of 5 in the case of I_N at its peak value). In addition, the cross sections I_U and I_N show clear peaks at $-t \simeq 0.25 - 0.35$ (GeV/c)² and $-t \simeq 0.45 - 0.55$ (GeV/c)², respectively. These structures were not seen in the Argonne analysis.

B. The mass dependence of solutions for $-t = 0.2 - 0.4$ (GeV/c)²

The mass dependence of moduli of normalized nucleon transversity amplitudes and cosines of relative phases in the mass interval $m = 812 - 972$ MeV and in the single t bin $-t = 0.2 - 0.4$ (GeV/c)² is shown in Fig. 6. Again, we present the results of independent analyses in the t - and s -channel helicity frames of the dimeson state.

In both channels the two solutions for P -wave moduli are similar while solution 2 for $|S|^2$ and $|\bar{S}|^2$ is substantially larger than solution 1. We note that the real solutions cluster around K^{*0} resonance in the mass interval $m = 872 - 932$ MeV where the statistics is highest. The amplitudes $|S|^2$, $|\bar{S}|^2$, $|N|^2$ and $|\bar{N}|^2$ are helicity frame invariant. A comparison of our results in the two channels confirms this expectation and provides also a useful self-consistency test of our amplitude analysis.

In the t -channel, the modulus $|L|^2$ peaks at $m \simeq 897$ MeV while $|\bar{L}|^2$ dips (solution 1) or is close to zero (solution 2). In the s channel such behavior is exhibited by the moduli $|U|^2$ and $|\bar{U}|^2$. The suppression of these amplitudes with recoil nucleon spin “up” at the resonant mass implies that $|L_0| \simeq |L_1|$ and $|U_0| \simeq |U_1|$ in the t and s channel, respectively. For a comparison we note that in the reaction $\pi^+ n \rightarrow \pi^+ \pi^- p$ at the same energy, the am-

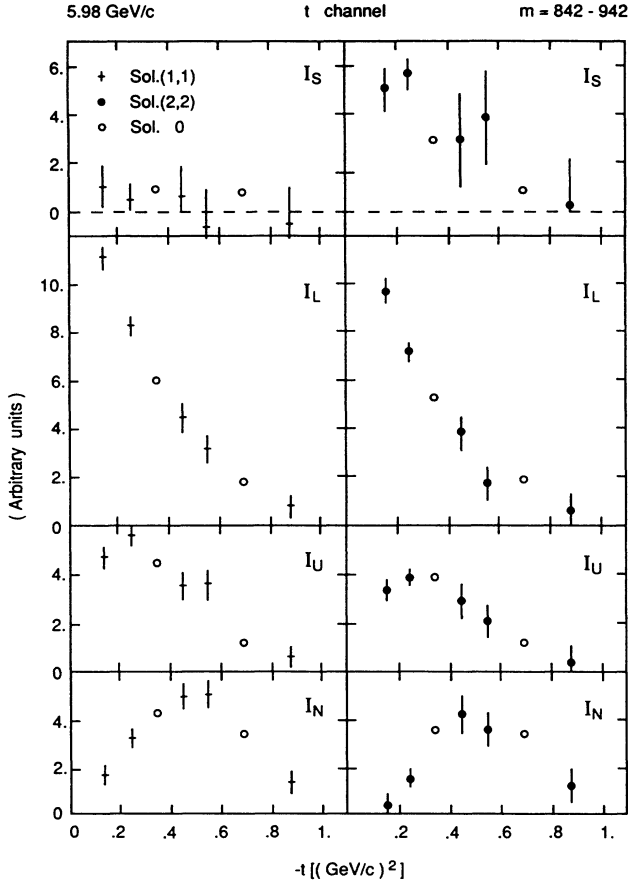


FIG. 5. The t dependence of unnormalized partial-wave cross sections for $m=842-942$ MeV at K^+ incident momentum of 5.98 GeV/c in the dimeson t -channel helicity frame. The units are arbitrary as in Fig. 3.

plitudes $|L|^2$ and $|\bar{L}|^2$ also peak and dip, respectively, at the resonance mass in the t channel, but $|L|^2 \approx |\bar{L}|^2$. A similar conclusion is true for $|U|^2$ and $|\bar{U}|^2$ in the s channel (Ref. [22], Figs. 5 and 12).

The calculated cosines of relative phases are helicity frame dependent. Looking first at $\cos\gamma_{LU}$ and $\cos\bar{\gamma}_{LU}$ we note that the results in the t - and s -channel helicity frames are similar but sign reversed. There seem to be also a considerable difference between solutions 1 and 2. Near resonant mass, solution 2 indicates that the pairs of amplitudes L, U and \bar{L}, \bar{U} are 180° out of phase in the t channel but are in phase in the s channel. Such behavior is also found for $\cos\gamma_{LU}$ and $\cos\bar{\gamma}_{LU}$ in the reaction $\pi^+n \rightarrow \pi^+\pi^-p$ at the same energy-momentum transfer (Ref. [22]). We also notice that $\cos\gamma_{SL}$ and $\cos\bar{\gamma}_{SL}$ in the t channel are similar to $\cos\gamma_{SU}$ and $\cos\bar{\gamma}_{SU}$ in the s channel. As well, $\cos\gamma_{SU}$ and $\cos\bar{\gamma}_{SU}$ in the t channel are similar to $-\cos\gamma_{SL}$ and $-\cos\bar{\gamma}_{SL}$ in the s -channel in this kinematic region.

In Fig. 7 we show the mass dependence of the partial-wave polarizations $\tau_A(1,2)$ and $\tau_A(2,1)$, $A=S,L,U,N$ in the t - and s -channel helicity frames. The solutions $\tau_A(1,1)$ and $\tau_A(2,2)$ show a similar behavior within the bounds of $\tau_A(1,2)$ and $\tau_A(2,1)$. While the two presented

solutions are similar for the P -wave polarizations they are markedly dissimilar for τ_S in the mass range of the K^{*0} resonance. The large values of τ_S, τ_L and τ_N in the t channel, in particular in the resonance mass range, indicate nontrivial contributions from nucleon helicity-nonflip amplitudes. The results for τ_S and τ_L again indicate the presence of “ A_1 - Z ” exchange contribution. The polarizations, τ_S and τ_L have a different behavior in $\pi^+n \rightarrow \pi^+\pi^-p$ reaction (Ref. [22], Fig. 9) where they are due to the interference of simpler “ A_1 ” and “ π ” exchange nucleon helicity amplitudes. However, it is remarkable that the polarization τ_U is small in both reactions in the same range of t . In the s channel, the roles of τ_L and τ_U are approximately reversed. The change of sign in τ_S, τ_N, τ_L (t channel) and τ_U (s channel) in the resonance mass region implies a change of sign of the relative phases of the corresponding relative phases in the pairs of nucleon helicity amplitudes, as is seen from Eq. (2.12).

It is of interest to present also the unnormalized amplitudes $|A|^2\Sigma$ and $|\bar{A}|^2\Sigma$ and the unnormalized partial-wave cross sections $I_A = \sigma_A \Sigma$. In these calculations we used for Σ our estimate of the acceptance corrected reaction cross section $d^2\sigma/dm dt$ given in Ref. [14] [Fig. 3(b)].

In Fig. 8 we show our results for the unnormalized amplitudes in the t channel. We see again that the S -wave amplitudes $|S|^2\Sigma$ and $|\bar{S}|^2\Sigma$ are small in solution 1 but large in the solution 2 in the K^{*0} mass range. The P -wave amplitude $|L|^2\Sigma$ peaks at 897 MeV while $|\bar{L}|^2\Sigma$ dips at this mass in both solutions. In solution 1, the amplitudes $|U|^2\Sigma$ and $|\bar{U}|^2\Sigma$ both peak at 887 MeV but the peak in $|U|^2\Sigma$ has a width which is narrower than the widths of peaks in $|\bar{U}|^2\Sigma$ and $|L|^2\Sigma$. In solution 2, the amplitude $|U|^2\Sigma$ is small while $|\bar{U}|^2\Sigma$ shows a broad structure. The amplitudes $|N|^2\Sigma$ and $|\bar{N}|^2\Sigma$ show some negative values, in particular in solution 2. We note that these negative values occur at one or two masses where the solutions for the moduli of S -wave amplitudes are also negative.

Figure 9 shows our results for unnormalized partial-wave cross sections in the t channel. The solution combination (1,1) yields an S -wave cross section $I_S(1,1)$ which has negative values in the K^{*0} resonance mass region while the P -wave partial wave cross sections $I_L(1,1)$, $I_U(1,1)$, and $I_N(1,1)$ all show the expected K^{*0} peak. However, the position of the K^{*0} peak varies with the dimeson helicity: it is at 897 MeV in $I_L(1,1)$ and at 887 MeV in $I_U(1,1)$ and $I_N(1,1)$.

The solution combination (2,2) yields the S -wave cross section $I_S(2,2)$ that shows a pronounced resonance structure at 887 MeV with a width of about 20 MeV. The P -wave partial wave cross sections now have more complex structures than they have in the solution combination (1,1). Only $I_L(2,2)$ shows a clear K^{*0} resonance shape at 897 MeV while $I_U(2,2)$ dips at 997 MeV and $I_N(2,2)$ shows a broad structure beyond the K^{*0} mass region. We notice that only the two cross sections $I_S(2,2)$ and $I_L(2,2)$ with the dimeson helicity $\lambda=0$ are large and show clear resonant shapes at these values of t .

It is tempting to reject the solution $I_A(1,1)$, $A=S,L,U,N$ on the basis of the negative values of $I_S(1,1)$ in the K^*0 mass region. In accepting only the solution combination (2,2) we have two cross sections $I_S(2,2)$ and $I_L(2,2)$ resonating at nearby masses of 887 and 897 MeV, respectively. Moreover, the relative phases between the amplitudes S,L and \bar{S},\bar{L} are approxi-

mately constant in the mass region of 870–900 MeV, as is seen in Fig. 6. On this basis we propose that our amplitude analysis indicates the possible existence of a scalar state $I=\frac{1}{2}0^+(887)$ with a width of approximately 20 MeV.

In the context of this proposal it is important to note that in our analysis the cross sections $I_U(2,2)$ and

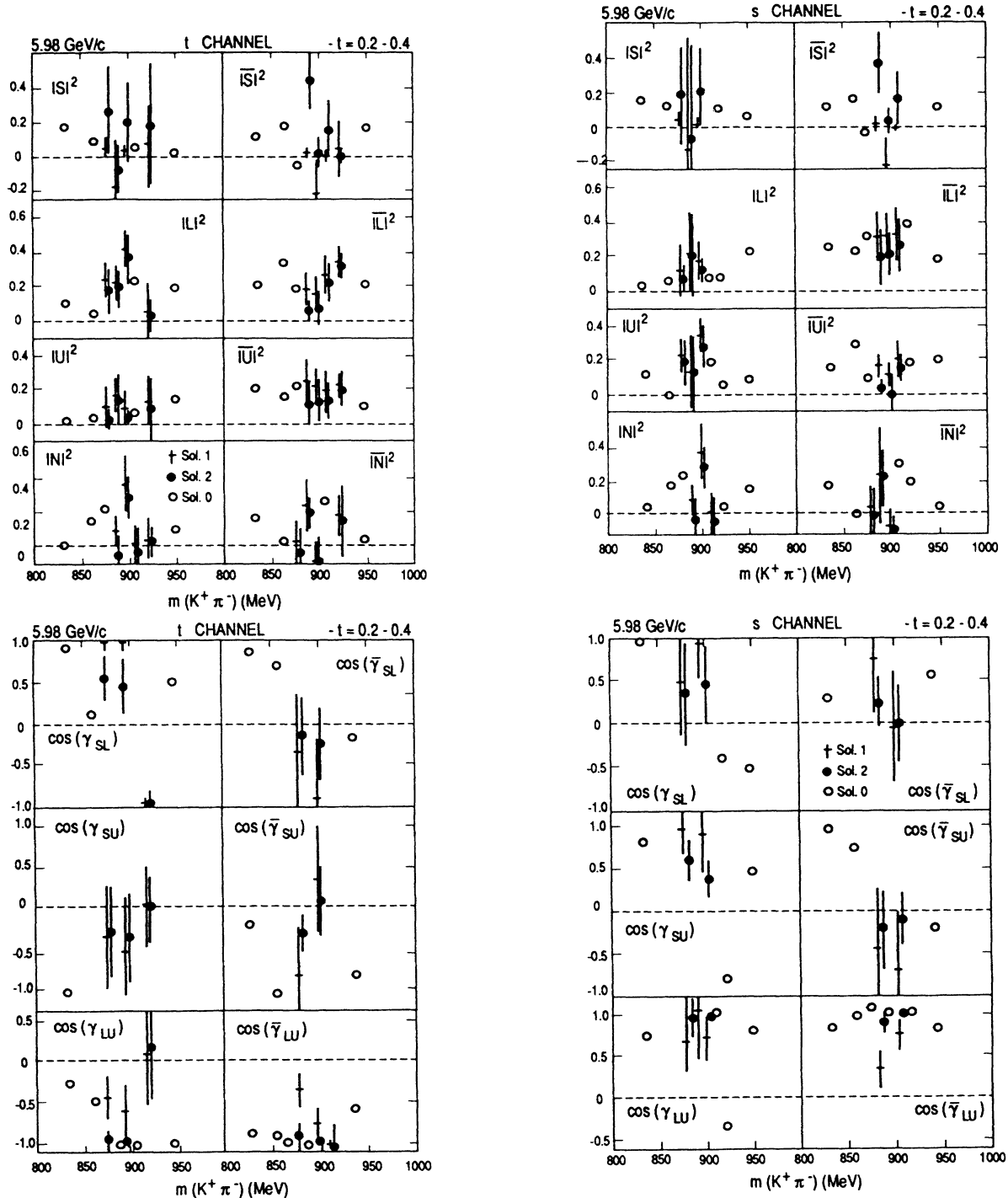


FIG. 6. The mass dependence of moduli squared of normalized nucleon transversity amplitudes and cosines of their relative phases for momentum transfers $-t=0.2-0.4$ (GeV/c)² at 5.98 GeV/c in the dimeson t - and s -channel helicity frames. The symbols are as in Fig. 1.

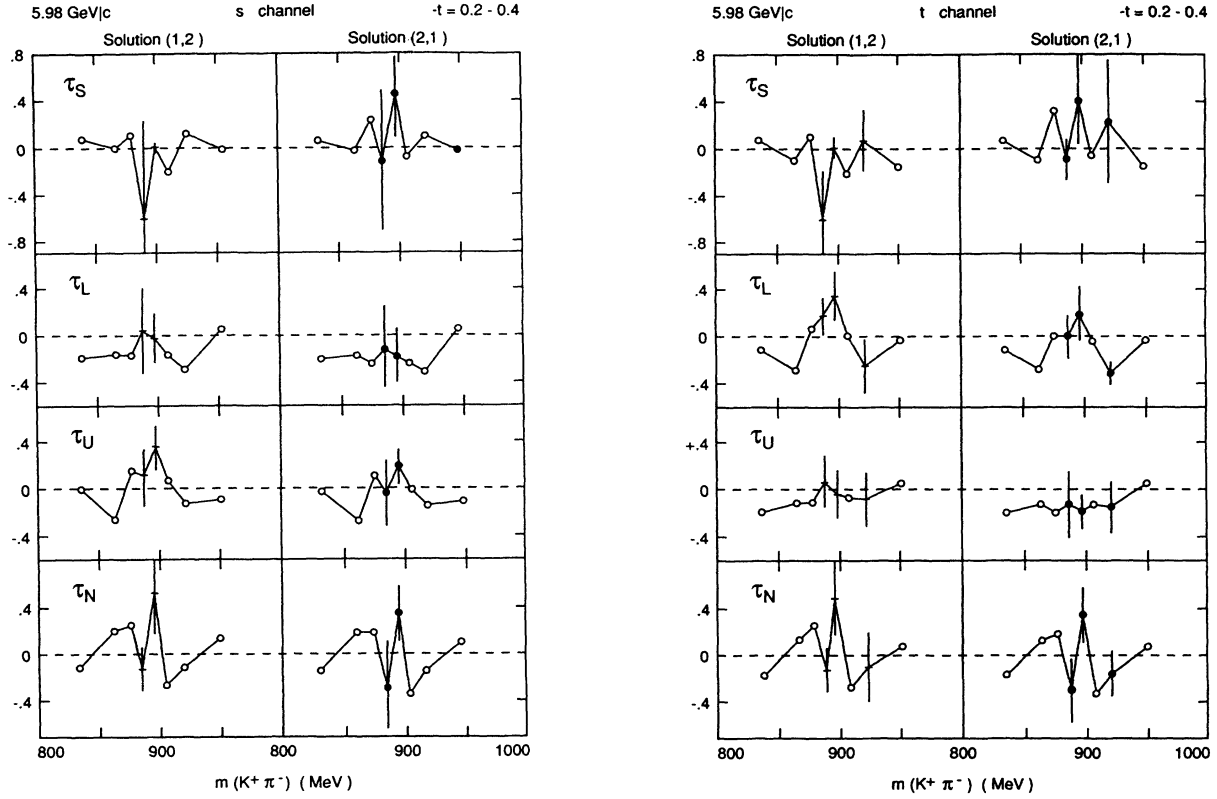


FIG. 7. The m dependence of partial-wave recoil polarization τ for $-t = 0.2 - 0.4$ (GeV/c)² at 5.98 GeV/c in the dimeson t - and s -channel helicity frames. Symbols as in Fig. 1.

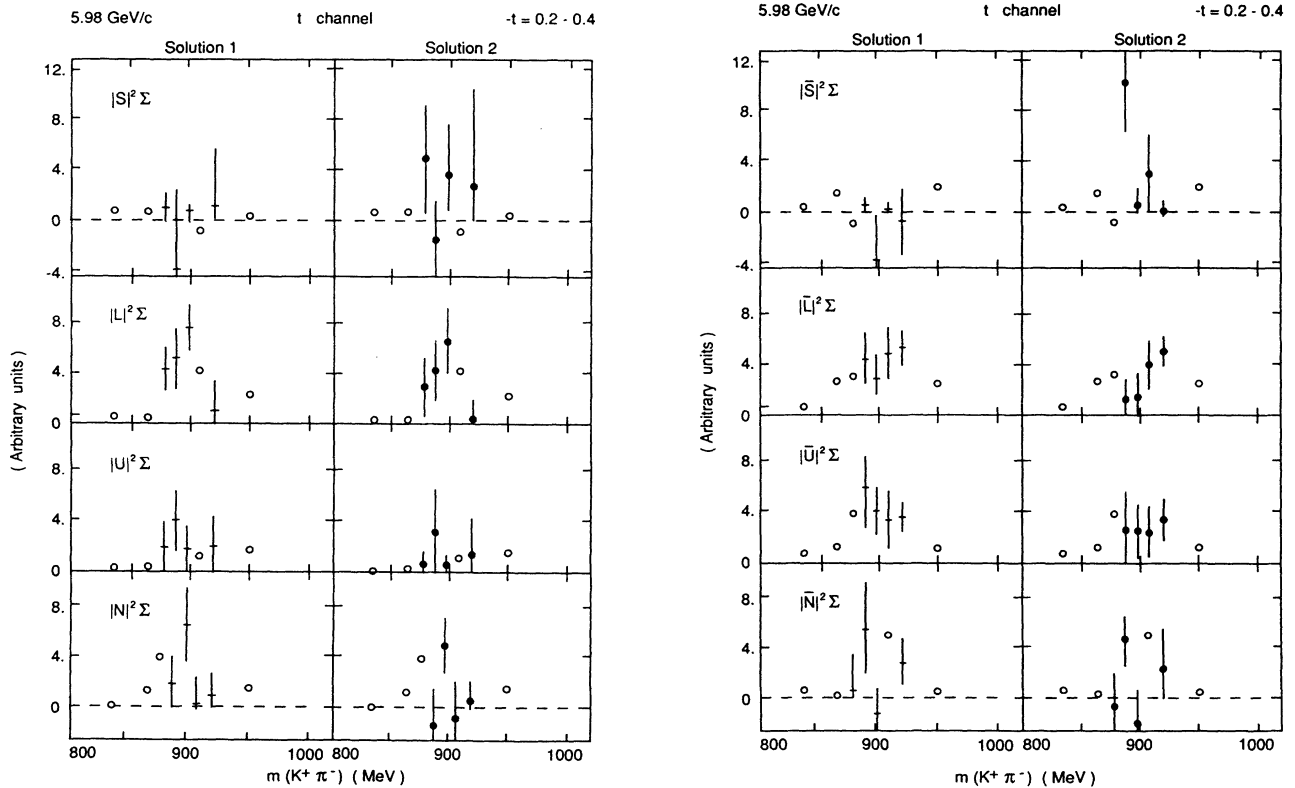


FIG. 8. The m dependence of moduli squared of unnormalized nucleon transversity amplitudes for $-t = 0.2 - 0.4$ (GeV/c)² in the t -channel helicity frame. The units are arbitrary and the same as in Fig. 3(b) of Ref. [14].

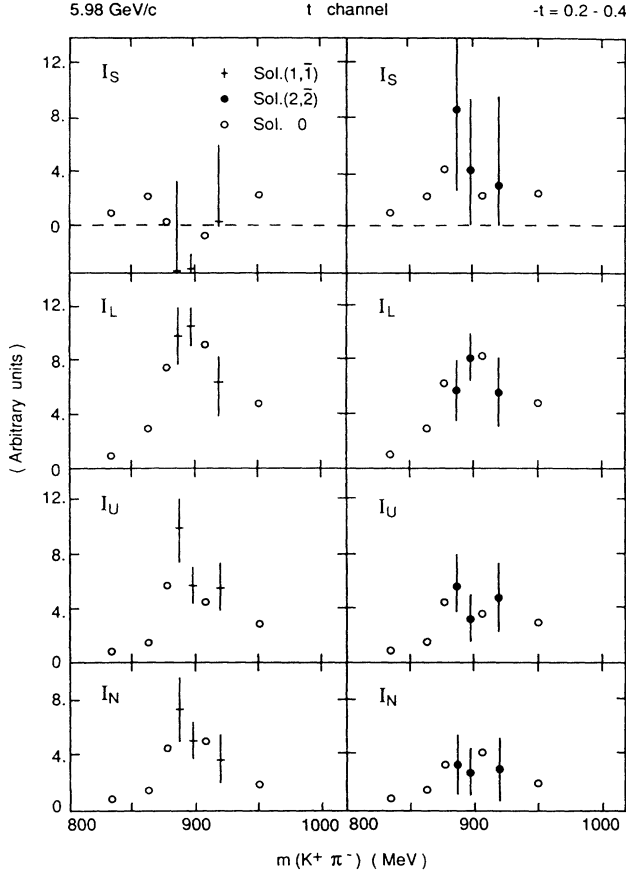


FIG. 9. The m dependence of unnormalized partial-wave cross sections for $-t=0.2-0.4$ $(\text{GeV}/c)^2$ in the t -channel helicity frame. The units are arbitrary and the same as in Fig. 8.

$I_N(2,2)$ do not have the expected uniform resonant shape to be shared by all P -wave cross sections. It is in this unexpected feature of the dimeson $\lambda=\pm 1$ cross sections I_U and I_N that our results differ from the previous analyses [27–29] which assumed a common resonant shape for all P -wave partial-wave cross sections I_L , I_U , and I_N in the $KN \rightarrow K\pi N$ reactions. This assumption is not well supported by our analysis of Saclay data on a polarized target. The use of this assumption in the past analyses may have led to the suppression of resonant structure in the S -wave cross section in the K^{*0} mass region. However, we note that a narrow scalar state $I=\frac{1}{2}0^+(890)$ with a width around 10 MeV was possibly seen in previous measurements of $K^-p \rightarrow K^-\pi^+p$ (Ref. [30]) and in the analysis of $K^+n \rightarrow K^+\pi^-p$ (Ref. [31]).

C. Test of additive quark model

We have published elsewhere [24] the results of applying our amplitude analysis in the binning (1.1) (t dependence) to test the validity of the additive quark model (AQM) on the level of amplitudes. The reactions $K^+n \rightarrow K^{*0}p$ and $pp \rightarrow \Delta^{++}n$ are both exotic in the s channel and exchange the same t -channel quantum numbers: $\pi-B$ and A_1-Z unnatural-parity exchanges and $A_2-\rho$ natural-parity exchanges. In general, the reaction

$pp \rightarrow \Delta^{++}n$ is described by 16 amplitudes. AQM reduces this number to 6 and relates these remaining amplitudes to those in $K^+n \rightarrow K^{*0}p$ at the same value of t . These relations between amplitudes lead to relations between SDM elements in the two reactions which include also two inequalities [24]. The test of those relations requires that certain SDM elements and other quantities in $K^+n \rightarrow K^+\pi^-p$ are known from the amplitude analysis of this reaction. The data are close to the predicted AQM equalities and satisfy a stringent cubic inequality. The observed small deviations from the AQM equalities may indicate nonadditive spin effects in hadron recombination [24].

D. On the constituent structure of $I=\frac{1}{2}0^+(887)$ state

In this subsection we shall assume the existence of the $I=\frac{1}{2}0^+(887)$ state and discuss briefly some possibilities for its constituent structure.

In the usual quark model, meson resonances are $q\bar{q}$ states. The mass M of a $q\bar{q}$ state increases with its angular momentum L as $M=M_0(2n+L)$ where n is the degree of radial excitation. The lowest mass scalar mesons are 3P_0 states with masses expected to be around and above 1000 MeV. This suggests that the state $I=\frac{1}{2}0^+(887)$ is unlikely to be a $q\bar{q}$ meson.

QCD introduces new gluonic degrees of freedom which lead to possible new types of hadrons. The MIT bag model [32] for four-quark states $q\bar{q}q\bar{q}$ predicts a strange scalar κ with the mass around 900 MeV and a broad width. However, models based on nonrelativistic potential seem to exclude $q\bar{q}q\bar{q}$ states [33]. Other possibilities based on QCD are monogluon and bigluon hybrid states $gq\bar{q}$ and $ggq\bar{q}$, and $K\pi$ molecule states. Predictions for strangeness-carrying hybrid scalar states are so far lacking.

Another possibility for the structure of $0^+(887)$ is based on a generalization of the concept of the hyperphoton. Several authors [32–41] discussed the possibility of a hypercharge carrying photon γ_Y and hypothesized its relation to the fifth force [42–44], a new weak intermediate-range force contributing to the macroscopic gravitational force. Such a new particle could be observed [42,43] in the decays $K^\pm \rightarrow \pi^\pm + \gamma_Y$.

In Fig. 10 we show the flavor-conserving $\bar{q}q\gamma$ coupling and the flavor-changing $\bar{s}d\gamma_Y$ coupling with the hyperphoton γ_Y carrying the strangeness of \bar{s} . The process

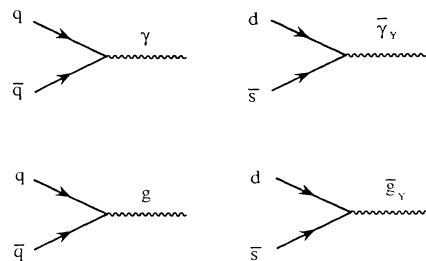


FIG. 10. Quark diagrams for $q\bar{q}$ annihilation into photon and gluon, and their generalization to hypercharge-carrying hyperphoton and hypergluon.

$\bar{s} \rightarrow d + \gamma_Y$ would be responsible for the decay $K^+ \rightarrow \pi^+ + \gamma_Y$.

In QCD, Lagrangian quark flavors are put in essentially by hand, and gluons do not change quark flavors. In Fig. 10 we show the usual $\bar{q}qg$ vertex and we introduce a QCD analogue of the hyperphoton which may be called a hypergluon g_Y . The hypergluon g_Y is a bicolor gauge field as is the gluon field but it changes the flavor of strange quarks. In Fig. 10 we show $d + \bar{s}$ annihilation into a hypergluon g_Y with strangeness +1.

In Fig. 11 we show a quark diagram in which the $K^+\pi^-$ state is produced by couplings $g\bar{u}u$ and $g_Y\bar{s}d$. Since both g and g_Y carry color, they can form a new hadron state gg_Y analogous to gluonium gg but one which carries a hypercharge. We propose to consider the possibility that the $0^+(887)$ state is the lowest-mass hypergluonium gg_Y . Since the hyper-gluonium carries no charge, the state $0^+(887)$ can be seen also in $K^-p \rightarrow K^-\pi^+n$ but not in $K^+n \rightarrow K^+\pi^0n$ and $K^-p \rightarrow K^-\pi^0p$ reactions.

IV. SUMMARY

We have performed a model-independent amplitude analysis of the reaction $K^+n_{\uparrow} \rightarrow K^+\pi^-p$ at 5.98 GeV/c using the Saclay data in two sets of binnings (1.1) and (1.2) to study the t dependence of pion production amplitudes in the K^{*0} mass region, and their dependence on a dimeson mass below 1000 MeV with a fixed $-t = 0.2 - 0.4$ (GeV/c)². The data on polarized target are best analyzed in terms of normalized nucleon transversity amplitudes (NTA's). In our kinematic region we worked with two S -wave and six P -wave amplitudes in both s - and t -channel dipion helicity frames.

Our analysis yields in each (m, t) bin two independent solutions for the moduli and cosines of relative phases of amplitudes in each of the two independent groups (3.1) and (3.2) of amplitudes with opposite nucleon transversities. The two solutions are similar, with the largest differences being in the S -wave moduli. In some (m, t) bins we obtained unphysical complex moduli. In such cases we presented their real parts. The occurrence of unphysical values for moduli and cosines is very likely due to the use of the unconstrained optimization of the

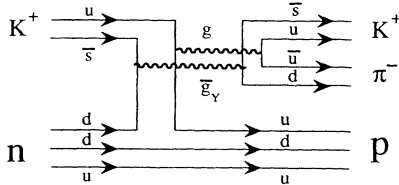


FIG. 11. Quark diagram contributing to the reaction $K^+n \rightarrow K^+\pi^-p$. The final dimeson state $K^+\pi^-$ is produced through the formation of gluon g and hypergluon g_Y . At the dimeson mass around 890 MeV a color neutral scalar hypergluonium state gg_Y is formed decaying into $K^+\pi^-$.

maximum-likelihood function in the data analysis and somewhat low statistics in these (m, t) bins.

We presented a detailed description of the behavior of amplitudes which show new and important features both in their t dependence and m dependence.

The t dependence of both solutions in the binning (1.1) shows contributions from nonzero nucleon helicity-nonflip amplitudes with “ $A_1 - Z$ ” exchange with phases different from the phases of nucleon helicity-flip amplitudes (“ $\pi - B$ ” exchange). The large differences between P -wave polarizations τ_L and τ_U in $\pi^+n_{\uparrow} \rightarrow \pi^+\pi^-p$ (Ref. [22]) and in $K^+n_{\uparrow} \rightarrow K^+\pi^-p$ (Fig. 2) indicate the presence of Z exchange with $I^G = 1^-$ and $J^{PC} = 2^{--}$.

A comparison of natural exchange amplitudes $|N|^2$ and $|\bar{N}|^2$ in the two reactions also shows interesting differences. While in both reactions $|\bar{N}|^2$ increases with $-t$ for $-t \gtrsim 0.5$ (GeV/c)², the amplitudes $|N|^2$ and $|\bar{N}|^2$ show a crossover at $-t \simeq 0.45$ (GeV/c)² in $\pi^+n \rightarrow \pi^+\pi^-p$. In contrast, in $K^+n \rightarrow K^+\pi^-p$ the amplitude $|N|^2 \simeq 0$ while $|\bar{N}|^2$ peaks at this value of t . These differences can be accounted for by the ρ -exchange contribution to the amplitudes $|N|^2$ and $|\bar{N}|^2$ in the $K^+n \rightarrow K^+\pi^-p$ reaction.

Elsewhere [24] we have used the results of our amplitude analysis for the t -dependence of amplitudes in the K^{*0} mass region to test additive quark model predictions relating reactions $K^+n \rightarrow K^{*0}p$ and $pp \rightarrow \Delta^{++}n$. The data are close to the predicted AQM equalities and satisfy a stringent cubic inequality [24]. Our tests provide the first experimental confirmation of the AQM on the level on amplitudes.

The mass dependence of moduli $|A|^2\Sigma$ and $|\bar{A}|^2\Sigma$, $A = S, L, U, N$ shows differences which reflect the important role of nucleon spin in pion production process. Within the mass range of the K^{*0} resonance, the t -channel amplitude $|L|^2\Sigma$ shows a peak while $|\bar{L}|^2\Sigma$ has a dip at 897 MeV. The structures of moduli within the mass range of K^{*0} are t dependent (see Fig. 2 in Ref. [21]) and provide entirely new information on the dynamics of K^{*0} production. We also note that the apparent position of the K^{*0} resonance for $-t = 0.2 - 0.4$ (GeV/c)² is 897 MeV for $|L|^2\Sigma$ but is lower in value 887 MeV for $|U|^2\Sigma$ and $|\bar{U}|^2\Sigma$.

The S -wave partial-wave cross section $I_S(1, 1)$ has negative values in the K^{*0} mass region while $I_S(2, 2)$ shows a large resonantlike structure. If the solution $I_S(1, 1)$ can be rejected for its negative values, then our amplitude analysis suggests the possible existence of a new scalar state $I = \frac{1}{2}0^+(887)$ with a width of approximately 20 MeV.

It appears unlikely that the $I = \frac{1}{2}0^+(887)$ state is a $q\bar{q}$ resonance. The possibility that it is a four-quark state $q\bar{q}q\bar{q}$ or a hybrid state $gq\bar{q}$ is also not very convincing although the MIT bag model predicts a $q\bar{q}q\bar{q}$ state at this mass. Our suggestion is to consider a generalization of the idea of a flavor-changing hyperphoton γ_Y and introduce an analogous flavor-changing hypergluon g_Y . Then the $I = \frac{1}{2}0^+(887)$ resonance could be a hypergluonium state gg_Y .

To conclude, we have demonstrated that new and important information on hadron dynamics and the proper-

ties of hadron resonances is provided by an amplitude analysis of pion production in $K^+n \rightarrow K^+\pi^-p$. Our results warrant new efforts to reach the level of amplitudes experimentally and with a high degree of precision in the new generation of experiments with spin at the recently proposed advanced hadron facilities [46–57].

ACKNOWLEDGMENTS

This work was supported by Fonds pour la Formation de Chercheurs et l'Aide à la Recherche (FCAR), Ministère de l'Éducation du Québec, Canada, and by Commissariat à l'Énergie Atomique, Saclay, France.

- [1] M. Fujisaki, Ph.D. thesis, 1978, Département de Physique des Particules Élémentaires, CEN Saclay, France.
- [2] M. Babou *et al.*, Nucl. Instrum. Methods **160**, 1 (1979).
- [3] L. van Rossum *et al.*, in *High Energy Physics with Polarized Beams and Polarized Targets*, Proceedings of the Third International Symposium, Argonne, Illinois, 1978, edited by G. H. Thomas, AIP Conf. Proc. No. 51 (AIP, New York, 1979), p. 478.
- [4] M. Svec *et al.*, in *High Energy Physics with Polarized Beams and Polarized Targets* [3], p. 491.
- [5] M. Fujisaki *et al.*, Phys. Lett. **80B**, 314 (1979).
- [6] M. Fujisaki *et al.*, Nucl. Phys. **B152**, 232 (1979).
- [7] M. Fujisaki *et al.*, Nucl. Phys. **B151**, 206 (1979).
- [8] M. Fujisaki *et al.*, Nuovo Cimento **99A**, 395 (1988).
- [9] A. de Lesquen *et al.*, in *Low and Intermediate Energy Kaon-Nucleon Physics*, edited by E. Ferrari and G. Violini (Reidel, Dordrecht, 1981), p. 289.
- [10] A. Itano *et al.*, in *High Energy Physics with Polarized Beams and Targets*, edited by C. Joseph and J. Soffer (Birkhauser, Boston, Cambridge, MA, 1981), p. 560.
- [11] A. de Lesquen *et al.*, Centre d'Études Nucléaires de Saclay, Internal Report No. DPhPE 82-01, 1982 (unpublished).
- [12] A. de Lesquen *et al.*, Phys. Rev. D **32**, 21 (1985).
- [13] A. Itano *et al.*, in *High Energy Physics with Polarized Beams and Targets* [10], p. 563.
- [14] A. de Lesquen *et al.*, Phys. Rev. D **39**, 21 (1989).
- [15] M. Svec *et al.*, in *Low and Intermediate Energy Kaon-Nucleon Physics* [9], p. 305.
- [16] M. Svec *et al.*, in *High Energy Physics with Polarized Beams and Targets* [10], p. 566.
- [17] M. Svec, in *Proceedings of the XXII International Conference on High Energy Physics*, Leipzig, East Germany, 1984, edited by A. Meyer and E. Wieczorek (Akademie der Wissenschaften der DDR, Zeuthen, 1985).
- [18] M. Svec, J. Phys. (Paris) Colloq. **46**, C2-281 (1985).
- [19] M. Svec, in *Hadron Spectroscopy-1985*, College Park, Maryland, edited by S. Oneda, AIP Conf. Proc. No. 132 (AIP, New York, 1985), p. 68.
- [20] M. Svec, A. de Lesquen, and L. van Rossum, in *Intersections Between Particle and Nuclear Physics*, Lake Louise, 1986, edited by Donald F. Geesaman, AIP Conf. Proc. No. 150 (AIP, New York, 1986), p. 1198.
- [21] M. Svec, A. de Lesquen, and L. van Rossum, Phys. Rev. D **42**, 934 (1990).
- [22] M. Svec, A. de Lesquen, and L. van Rossum, Phys. Rev. D **45**, 55 (1992).
- [23] A. de Lesquen *et al.* [11], pp. 103-110.
- [24] M. Svec, A. de Lesquen, and L. van Rossum, Phys. Lett. B **220**, 653 (1989).
- [25] G. Lutz and K. Rybicky, Max Planck Institute, Munich, Internal Report No. MPI-PAE/Exp. EI.75, 1978 (unpublished).
- [26] I. Sakrejda, Ph.D. thesis, Institute of Nuclear Physics, Cracow, 1984, Report No. 1262/PM.
- [27] A. B. Wicklund *et al.*, Phys. Rev. D **17**, 1197 (1978).
- [28] P. E. Schlein, Phys. Rev. Lett. **19**, 1052 (1967).
- [29] P. Estabrooks *et al.*, Nucl. Phys. **B133**, 490 (1978).
- [30] P. Lauscher *et al.*, Nucl. Phys. **B86**, 185 (1975).
- [31] A. Firestone *et al.*, Phys. Rev. D **5**, 2183 (1972); M. G. Bowler *et al.*, Nucl. Phys. **B126**, 31 (1977).
- [32] R. L. Jaffe, Phys. Rev. D **15**, 267 (1977); **15**, 281 (1977).
- [33] J. Weinstein and N. Isgur, Phys. Rev. D **27**, 588 (1983).
- [34] J. S. Bell and J. K. Perring, Phys. Rev. Lett. **13**, 348 (1964).
- [35] J. Bernstein, N. Cabibbo, and T. D. Lee, Phys. Lett. **12**, 146 (1964).
- [36] S. Weinberg, Phys. Rev. Lett. **13**, 495 (1964).
- [37] H. Galic, Z. Phys. C **29**, 1339 (1985).
- [38] M. Suzuki, Phys. Rev. Lett. **56**, 1339 (1986).
- [39] S. H. Aronson *et al.*, Phys. Rev. Lett. **56**, 1342 (1986).
- [40] C. Bouchiat and J. Ilionopoulos, Phys. Lett. **169B**, 447 (1986).
- [41] M. Lusignoli and A. Pugliese, Phys. Lett. B **171**, 468 (1986).
- [42] E. Fishbach *et al.*, Phys. Rev. Lett. **56**, 3 (1986); **56**, 1427 (E) (1986).
- [43] E. Fishbach *et al.*, Ann. Phys. (N.Y.) **182**, 1 (1988).
- [44] S. Aronson *et al.*, Brookhaven National Laboratory Report No. BNL-41475, 1988 (unpublished).
- [45] Y. Asano *et al.*, Phys. Lett. **107B**, 159 (1981).
- [46] E. Vogt, Nucl. Phys. **A450**, 473c (1986); J. Domingo, *ibid.* **A450**, 473c (1986); G. T. Garvey, *ibid.* **A450**, 539c (1986).
- [47] *Canadian KAON Factory* (TRIUMF, Vancouver, 1985).
- [48] *Physics and a Plan for a 45 GeV Facility* [LANL Report No. LA-10720-MS, Los Alamos, 1986 (unpublished)].
- [49] *Proceedings of the International Conference on a European Hadron Facility*, Mainz, Germany, 1986, edited by T. Walcher [Nucl. Phys. **B279**, 2 (1987)].
- [50] *International Workshop on Hadron Facility Technology*, Proceedings, Los Alamos, New Mexico, 1987, edited by H. A. Thiessen [LANL Report No. LA-11130-C, Los Alamos, 1987 (unpublished)].
- [51] Japanese Hadron Facility, in *International Workshop on Hadron Facility Technology* [50], p. 67.
- [52] *Proceedings of Workshop on Hadron Spectroscopy at the Kaon Factory*, Vancouver, Canada, 1989 (TRIUMF Report No. TRI-89-4, Vancouver, 1989).
- [53] *Physics at KAON*, edited by D. Frekers, D. R. Gill, and J. Speth (Springer-Verlag, Berlin, 1990); Z. Phys. C **46**, S1 (1990).
- [54] *Multi-user Hadron Spectrometer Workshop*, edited by M. Comyn, TRIUMF Report, 1990 (unpublished).
- [55] *Workshop on Science at the KAON Factory*, edited by D. R. Gill [TRIUMF Report, 1990 (unpublished)].
- [56] G. Preparata, in *Intense Hadron Facilities and Antiproton Physics*, Conference Proceedings, edited by T. Bressani, F. Iazzi, and G. Pauli (SIF, Bologna, 1990), Vol. 26, 89.
- [57] M. Svec, in *High-Energy Spin Physics: Eighth International Symposium*, edited by Kenneth J. Heller, AIP Conf. Proc. No. 187 (AIP, New York, 1989), Vol. 2, p. 1181.